IJST EXPLORE International Journal of Science and Technology
CENTRE OF PROFESSIONAL RESEARCH PUBLICATIONS
ISSN 2049-7318

International Journal of Science and Technology Volume 1 No. 6, June, 2012

Anti-Angiogenic Activity of Naturally Occurring Lower Size Isoforms of Buffalo Pituitary Prolactin

Jaeok Lee, Rajesh Chaudhary, Kambadur Muralidhar
Hormone Research Laboratory, Department of Zoology, University of Delhi, Delhi, India

ABSTRACT

The lower size (14 kDa-18 kDa) isoforms of buffalo pituitary prolactin (PRL), separated from the monomer and higher size forms, has anti-angiogenic activity in human endothelial cell migration assay and chick embryo chorioallantoic membrane (CAM) analysis. The isoforms also showed 35 times less immunoreactivity than the hormone monomer. There was no 16 kDa isoform of buffalo PRL. This is the first demonstration that the PRL fragments, which are physiologically cleaved in pituitary glands and biochemically purified, inhibit angiogenesis.

Keywords: *buffalo PRL isoform, Anti-angiogenesis, microheterogeneity*

1. INTRODUCTION

PRL from buffalo pituitaries was first purified in 1988 (Muralidhar, *et al.*, 1988). For over 20 years, biochemical and biological studies have been made to understand buffalo PRL (buPRL). The N-/C-terminal amino acids of the hormone were 'Thr' (Chadha, *et al.*, 1991; Khurana and Muralidhar, 1997) and 'Cys' (Panchal and Muralidhar, 2010), respectively. The molecular size of buPRL monomer is 22,664 Da as determined by MALDI-TOF analysis (Panchal and Muralidhar, 2008). Enhancement of Nb2 rat lymphoma cell proliferation by the hormone has been studied (Khurana and Muralidhar, 1997).

This hormone has micro-heterogeneous forms. Buffalo and sheep PRL have been reported, to have an usual post-translational modification in the form of Tyr-*O*-sulfation (Kolhi, *et al*., 1987; 1988; Chadha, *et al.*, 1991), to exhibit lower sized (19 kDa and 13 kDa) forms (Khurana and Muralidhar, 1997) and show partial glycosylation (Khurana and Muralidhar, 1997). However, the biological functions of the heterogeneous forms if any are not known yet.

Here we investigated that the naturally occurring lower size isoforms of buPRL. They were found to exhibit anti-angiogenic activity in endothelial cell migration and CAM assays. Moreover, the isoforms had much less immunoreactivity against buPRL antisera than the hormone monomer. Furthermore, *in silico* method, the homology modeling of buPRL was carried out. The sites of sulfation and phosphorylation were predicted.

2. MATERIALS AND METHODS

2.1 Materials

Buffalo *(Bubalus bubalis)* pituitary glands were obtained from a local slaughter house. Sephacryl S-200 beads were from Pharmacia, USA. Goat anti-rabbit IgG horseradish peroxidase (HRP) conjugate were from Genei, India. Coomassie brilliant blue G-250 was purchased from Merck, India. 4-chloro-1-naphthol and ortho-phenylenediammine (OPD) were obtained from Sigma Chemical Company, St. Luise, USA. Microconcept 1 K cut off centrifugal device (Omega^{TM} membrane) was purchased from Pall Life Sciences, USA. All the other reagents were of analytical grade.

2.2 Methods

2.2.1 Purification of buPRL Monomer from Discarded Acid Pellet

Extraction

Freshly frozen buffalo pituitary glands were homogenized in 150 mili mol l^{-1} $(NH_4)_2SO_4$, 1 mili mol l^{-1} PMSF with a blender. The homogenate was stirred, pH adjusted to pH 4.0, let stand for 1hr and centrifuged at 2,300 xg for 30 min (Papkoff *et al*., 1965). The acid pellet was suspended in 250 mili mol l^{-1} $(NH_4)_2SO_4$ and set to pH 5.5 (Ellis S, 1961). It was then stirred and centrifuged at 9,000 xg for 30 min (Khurana and Muralidhar, 1997). The residue (residue C) was taken for extraction in 70% v/v pre-chilled ethanol, pH 9.0-10.0. The supernatant obtained after centrifugation was adjusted to pH 5.5. The pH 5.5 precipitate was collected by centrifugation ((AP)P-I 70). The supernatant was stirred with two volumes of chilled 98 % v/v ethanol at -20 ^{0}C for 2 hrs, and the precipitate collected by centrifugation ((AP)P-I 90-70). The (AP)P-I fraction was dissolved in 70 v/v % chilled ethanol (pH 9.0-10.0) again followed by precipitation at pH 5.5 ((AP)P-II 70) again. This procedure was repeated twice. The final pellets ((AP)P-III 70) and (AP)P-I 90-70 were dissolved in 100 mili mol l^{-1} NH_4HCO_3, and stored lyophilized.

Sephacryl S-200 Gel Filtration

APP-I and (AP)P-III 70 dissolved in 100 mili mol l^{-1} NH_4HCO_3 were loaded onto separate column (4.52 cm X 92 cm) of Sephacryl S-200 resin equilibrated with 100 mili

mol l^{-1} NH_4HCO_3. 5.7 mL fractions were collected at a flow rate of 33 mL/hr and monitored for absorbance at 280 nm. Peak aliquots were pooled and lyophilized and then stored at -20 ^{0}C.

Protein Estimation

Lowry's method (Lowry, *et al.*, 1951) and Bradford's method (Bradford MM, 1976) were performed for protein estimation.

SDS-PAGE and Immunoblot Analysis

SDS-PAGE and immunoblot analysis were performed with modified Laemmli's (Laemmli UK, 1970) and Towbin's (Towbin, *et al*., 1979) methods, respectively. For immunoblot analysis, antigen-antibody complexes were detected by using the substrate, 4-chloro-1-naphthol along with goat anti-rabbit gamma-globulin conjugated to horseradish peroxidase.

Gel Staining and Destaining

For detecting the separated proteins, the gel was stained with 0.12 % w/v coomassie brilliant blue G-250 solution (Candiano, *et al.*, 2004), and then destained with destaining solution (20 % v/v acetic acid/ 10 % v/v methanol).

2.2.2 Anti-angiogenic Activity Analysis

Cell Culture

EAhy926, (Edgell, *et al.*, 1983) was maintained in DMEM, supplemented with 10 % v/v fetal bovine serum, penicillin (100 U/mL), and streptomycin (50 pg/mL), at 37 ^{0}C/5 % CO_2 (Astec, Japan).

Wound Healing Cell Migration Assay

Cell migration was observed using the wound healing method (Staton, *et al.*, 2004). After 12~16 hrs from seeding when EAhy926 cells were confluent, a cross linear wound was created by scratching the monolayer with a 1 mm wide sterile plastic scraper. The cells were treated with protein or peptide, and incubated for 0 hr, 4 hrs and 8 hrs. Bright-field images were acquired using a Nikon CoolPix digital camera adapted to an inverted bright-field microscope with 40X magnifications. The rate of wound healing was quantified from the images using 'ImageJ', (Release Alpha 4.0 3.2 and Adobe Photoshop version 6.0.)

Early stage CAM assay

CAM assay was performed using 4^{th}~6^{th} day incubated eggs (Hazel SJ, 2003). 4^{th}~6^{th} day incubated eggs were open north polar area (2 cm X 2 cm) and gently plated onto dishes under sterile conditions. Disks contacting target factors including control (1X PBS) were placed on the vascular bed of egg yolks, and the eggs were incubated for 8hrs. Images were taken at a 20X magnification using a Nikon CoolPix digital camera adapted to a stereo-microscope after 0 hr, 4 hrs and 8 hrs of incubation. Analysis of angiogenesis was performed by using Adobe Photoshop 7.0 and 'AngioQuant' software (Niemisto, *et al.*, 2005).

Statistical Analysis

All experiments were performed in triplicate (n=3) unless otherwise specified. The data are presented as means ± standard error (SE). The data were analyzed using a one-way ANOVA test and *t*-test as appropriate (Sigma Stat software). $p < 0.05$ was considered statistically significant.

2.2.3 Enzyme Linked Immunobsorbent Assay (Elisa)

According to Khurana and Muralidhar's procedure (1997), 1, 10, 100, 1,000 and 10,000 ng of buPRL monomer and (AP)P-I 90-70 per 100 uL were coated in each well for ELISA with buPRL antiserum (1:1,000). Antigen-antibody complexes were detected by using the substrate, OPD along with goat anti-rabbit gamma-globulin antibody conjugated to HRP. The 96-well ELISA plate with antigen-antibody complexes was read at 490 nm using ELISA reader (ECIL, India).

In Silico Analysis

The primary sequence of buPRL (GeneBank accession no. ABY61078) was used, for building tertiary structure, for analyzing physico-chemical properties, for predicting post-translational modification, and for searching the binding site.

The tertiary structure of the hormone was modeled with a template1rw5A (PDB accession number) (Teilum, *et al.*, 2005) by Automated Mode in SWISS-MODEL server (Schwede, *et al.*, 2003; Arnold, *et al.*, 2006). The display and analysis of tertiary structure were done with Swiss-PdbViewer DeepView v4.0 (Guex and Peitsch, 1997).

ExPASy Proteomics tools (Gasteiger, *et al.*, 2005) were used for analysis of physico-chemical characteristics and prediction of tyrosine-*O*-sulfate site and phosphorylation site.

3. RESULTS AND DISCUSSION

3.1 Purification of Buffalo PRL Monomer from a Discarded Acid Pellet

The APP-I, a semi-pure buPRL (Chaudhary, et al., 2004), has higher sized forms (>34.9 kDa, 34.9 kDa and 25.9 kDa (26 K)) and lower sized forms (18.4 kDa (18 K), 14.5 kDa (14 K) and <14.5 kDa) as well as buPRL monomer (23.4 kDa) (Figure 1, A~C). The lower sized forms, approximately 18 K and 14 K under non-reducing conditions transform into 19 K and 13 K bands under reducing conditions (Khurana and Muralidhar, 1997). The 26 K under non-reducing condition may be the isoform nicked in the large loop of intact form but with intact disulfide bonds (Mittra I, 1980a; 1980b). Khurana and

Muralidhar (1997) reported that 25 K buPRL (under non-reducing condition of SDS-PAGE) disappeared under reducing condition of the gel.

The size isoform mixture, APP-I could be separated by differential alcohol precipitation (Figure 2). APP-I 70 (higher sized form mixture) and APP-I 90-70 (lower sized form mixture) were subjected to SDS-PAGE analysis (Figure 1, D and F). The lower sized form mixture, APP-I 90-70, was confirmed to be free from higher sized forms by immunoblotting analysis (Figure 1, E, L4'). The reason for the successful separation of the two different sized mixtures had different pI. Buffalo PRL monomer has pI 5.1~5.45 (Chadha, *et al*., 1991). The higher sized forms and monomer are probably soluble in the alkaline ethanol. The buPRL lower sized peptides had opposite property.

3.2 Anti-angiogenic Activity of (AP) P-I 90-70 Fraction, Lower Size Isoforms Mixture

It has been known that N-terminal 16K PRL fragment had an inhibitory effect on angiogenesis, the formation of new blood vessels (Folkman and Shing, 1992), in rat (Ferrara, *et al*., 1991) and in human (Clapp, *et al*., 1993) both *in vitro* and *ex vivo*. Thus, it is interesting whether the lower size forms mixture including 18K and 14K size forms (Figure 1, A), naturally occurring PRL peptides, has the anti-angiogenic activity or not. For the query, (AP)P-I 90-70 fraction was tested with endothelial cell migration assay (*in vitro*) and chick egg yolk membrane assay (*ex vivo*) (Figure 3). Approximately 7 % inhibition of cell migration compare to control was observed after 4 hrs and 8 hrs, when 30 pg/ml of (AP)P-I 90-70 was treated to human immortalized umbilical vein endothelial cells, EAhy926. The development of the vessel on chick egg yolk membrane was inhibited by the same concentration of (AP)P-I 90-70. These results can be the proof that the physiologically (*in vivo*) cleaved buPRL fragments had an anti-angiogenic function.

As it is known that C-terminal 16 K hPRL does not have the biological activity, the present PRL size isoforms could be majorly N-terminal fragments. If C-terminal fragments were in the isoforms mixture, their presence is could not have affected the activity in the N-terminal side peptides.. Or those fragments may include specific anti-angiogenic active site. This (AP)P-I 90-70 fraction needs to be further characterized.

Struman, *et al*. (1999) reported that intact human PRL, GH and PL exhibited angiogenic activity. However, our results indicate unequivocally that the buPRL monomer had no significant stimulatory or inhibitory effect on blood vessel formation in CAM and endothelial cell migration (Figure 3, A and D).

3.3 Immunoreactivity of buPRL Monomer and the Lower Sized Isoforms Mixture

The comparative immunoreactivity of the buPRL size isoforms was analyzed by ELISA. buPRL and bovine serum albumin (BSA) were used as a positive and negative controls, respectively. The immune activity of buPRL monomer was approximately thirty five times higher than that of the lower sized mixture, (AP)P-I 90-70 (Figure 4 and Table 2). Lower sized PRL forms have low immunoreactivity with PRL monomer antibodies (Clapp, *et al*., 1988). This result can be understood that lower sized forms have less binding affinity to PRL antibodies than buPRL monomer which has 3 epitopes (data not shown). It should also be noted that conversely the immunoreactivity of 16K PRL fragment against 16K specific polyclonal antibodies in RIA was reported to be hundred times more than that of intact PRL (Clapp, *et al*., 1994). Obviously, the 16K fragment after its cleavage from intact PRL by virtue of conformational alterations must have exhibited different antigenic epitopes than the intact PRL.

3.3.1 In Silico Studies of buPRL

Physico-chemical property of buPRL (Thr13 to Cys211 of ABY61078) was analyzed with 'Protparam' of ExPASy tools. buPRL consisted of 199 amino acids had 22678.8 Da as molecular mass and a pI 5.63. The predicted molecular mass and pI appear a little higher than the practical data, 22664.786 Da by MALDI-TOF (Panchal and Muralidhar, 2008) and 5.1~5.45 of pI range obtained by analytical isoelectric focusing (Chadha, *et al*., 1991).

3.3.2 Tyrosine-O-sulfate of buPRL Monomer

Earlier study proved Tyr-*O*-sulfation of buPRL (Kolhi, *et al*., 1987; 1988; Chadha, *et al*., 1991). Hence the prediction of Tyr-*O*-sulfate site in the sequence of buPRL monomer was performed with 'sulfinator (Monigatti, *et al*., 2002)' of ExPASy proteomics tools. Among eight Tyr residues, two (Tyr28 and Tyr96) were found to have potential for sulfation (Figure 5, A). The more significant candidate, however, was Tyr28 (E-value 3.7), located in the first α-helix set on superficial area (Figure 5, A).

The sulfation at Tyr residue in buPRL seems to be not uniform. Approximately 0.345 sulfur atoms per buPRL monomer, after removing 13 sulfurs used for Cys and Met (Panchal and Muralidhar, 2008), may be used for sulfation of tyrosine, that is, about a third of buPRL monomer can be in the Tyr-*O*-sulfated form. Sulfation of Tyr seems to have less chance than that of glycosylated form in buPRL (Kolhi, *et al*., 1987).

3.3.3 Phosphorylation of buPRL Monomer

The phosphorylation sites of Ser, Thr and Tyr residues in buPRL monomer were, also, predicted with 'NetPhos (Blom, *et al*., 1999)' of ExPASy Proteomics tools. The candidates of phosphorylation site were found to be six among fifteen Ser residues, Ser14, Ser26, Ser34, Ser90, Ser179 and Ser180, four among nine Thr residues, Thr1, Thr65, Thr75 and Thr158, and four among eight Tyr residues, Tyr44, Tyr96, Tyr165 and Tyr195 (Figure 5, B). Among the above sites, Ser26, Ser34 and Ser90 reported in bPRL can be significant candidates, and Ser90 conserved in PRL, GH and PL (Kim and Brooks, 1993).

In PRL, it is considered that phosphorylated isoform has a unique biological function such an autocrine regulation in lactotroph secretion (Ho, *et al.*, 1989), and also less cell proliferative activity (against Nb2 lymphoma cells) than the non-phosphorylated form (Wang and Walker, 1993). The rate of PRL phosphorylation was reported 20 ~ 80 % in bovine (Kim and Brooks, 1993).

The phosphorylation of PRL decreases receptor binding by changing the hormone structure conformation (Kim and Brooks, 1993). The Tyr28, the candidate of Tyr-*O*-sulfation, was not selected for phosphorylation, but Tyr96, which is not a significant candidate of Tyr-*O*-sulfation, appeared as a significant candidate for phosphrylation.

4. CONCLUSION

The physiologically cleaved buPRL peptide fragments had anti-angiogenic activity. This function was verified with endothelial migration and CAM assay and in very low concentration.

REFERENCES

[1] Arnold K, Bordoli L, Kopp J & Schwede T 2006 The SWISS-MODEL workspace: a web-based environment for protein structure homology modeling. *Bioinformatics* **22** 195-201.

[2] Blom N, Gammeltoft S & Brunak S 1999 Sequence and structure-based prediction of eukaryotic protein phosphorylation sites. *Journal of Molecular Biology* **294** 1351-1362.

[3] Bradford MM 1976 A rapid and sensitive method for the quantitation of microgram quantities of protein utilizing the principle of protein-dye binding. *Analytical Biochemistry* **72** 248-754.

[4] Candiano G, Bruschi M, Musanta L, Santucci L, Ghiggeri GM, Carnemolla B, Orecchia P, Zardi L & Righetti PG 2004 Blue silver:A very sensitive colloidal Coomassie G-250 staining for proteome analysis. *Electrophoresis* **25** 1327-1333.

[5] Chadha N, Kohli R, Kumari GL & Muralidhar K 1991 Physico-chemical and immunological characteristics of pituitary prolactin from water buffaloes (*Bubalus bubalis*). *Molecular Cellular Biochemistry* **105** 61-71.

[6] Chaudhary R, Lee JO & Muralidhar K 2004 Simultaneous isolation of prolactin and growth hormone from “discarded acid pellet” obtained from buffalo pituitaries. *Preparative Biochemistry and Biotechnology* **34** 331-343.

[7] Clapp C, Martial JA, Guzman RC, Rentier-Delrue F & Weiner RI 1993 The 16-kilodalton N-terminal fragment of human prolactin is a potent inhibitor of angiogenesis. *Endocrinology* **133** 1292-1299.

[8] Clapp C, Sears DS, Russell DH, Richards J, Levay-Young BK & Nicoll CS 1988 Biological and immunological characterization of cleaved and 16K forms of rat prolactin. *Endocrinology* **122** 2892-2898.

[9] Clapp C,Torner L, Gutie’rrez-Ospina G, Alca’ntara E, Lo’pez-Go’mez FJ, Nagano M, Kelly PA, Meji’a S, Morales MA & Marti’nezde la Escalera G 1994 The prolactin gene is expressed in the hypothalamicneurohypophyseal system and the protein is processed into a 14-kDa fragment with activity like 16-kDa prolactin. *Proceeding of the National Academy of Sciences* **91** 10384–10388.

[10] Edgell C-JS, McDonald CC & Graham JE 1983 Permanent cell line expressing human factor VIII-related antigen established by hybridization. *Proceeding of the National Academy of Sciences* **80** 3734-3737.

[11] Ellis S 1961 Studies on the serial extraction of pituitary proteins. *Endocrinology* **69** 554-570.

[12] Ferrara N, Clapp C & Weiner R 1991 The 16K fragment of prolactin specifically inhibits basal or fibroblast growth factor stimulated growth of capillary endothelial cells. *Endocrinology* **129** 896-900.

[13] Folkman J & Shing Y 1992 Angiogenesis. *Journal of Biological Chemistry* **267** 10931–10934.

[14] Gasteriger E, Hoogland C, Gattiker A, Duvaud S, Wilkins MR, Appel RD & Bairoch A 2005 Protein identification and analysis tools on the ExPASy server. In *The Proteomics Protocols Handbook*, pp571-607. Eds JM Walker. New Jersey: Humana Press Inc.

[15] Guex N & Peitsch MC 1997 SWISS-MODEL and the Swiss-PdbViewer: An environment for comparative protein modeling. *Electrophoresis* **18** 2714-2723.

[16] Hazel SJ 2003 A novel early chorioallantoic membrane assay demonstrates quantitative and qualitative changes caused by antiangiogenic substances. *Journal of Laboratory and Clinical Medicine* **141** 217-228.

[17] Ho TWC, Greenan JR & Walker AM 1989 Mammotroph autoregulation: the differential roles of the 24K isoforms of prolactin. *Endocrinology* **124** 1507-1514.

[18] Khurana S & Muralidhar K 1997 Heterogeneity in buffalo pituitary prolactin. *Molecular Cellular Biochemistry* **173** 1-15.

[19] Kim BG. & Brooks CL 1993 Isolation and characterization of phosphorylated bovine prolactin. *Biochemical Journal* **296** 41-47.

[20] Kohli R, Chadha N & Muralidhar K 1987 Are sheep and buffalo prolactins sulfated? *Biochemical and Biophysical Research Communications* **149** 515-522.

[21] Kohli R, Chadha N & Muralidhar K 1988 Presence of tyrosine-o-sulfate in sheep pituitary prolactin. *FEBS Letters* **242** 139-143.

[22] Laemmli UK 1970 Cleavage of structure proteins during the assembly of the head of bacteriophage T4. *Nature* **227** 680-685.

[23] Lowry OH, Rosenbrough NJ, Farr AL & Randall RJ 1951 Protein measurement with the folin phenol reagent. *Journal of Biological Chemistry* **193** 265-275.

[24] Mittra I 1980a A novel "cleaced PRL" in the rat pituitary: Part I biosynthesis, characterization and regulatory control. *Biochemical and Biophysical Research Communications* **95** 1750-1759.

[25] Mittra I 1980b A novel "cleaced PRL" in the rat pituitary: Part II *in vivo* mammary mitogenic activity of its N-terminal 16K moiety. *Biochemical and Biophysical Research Communications* **95** 1760-1780.

[26] Monigatti F, Gasteiger E, Bairoch A & Jung E 2002 The sulfinator: predicting tyrosine sulfation sites in protein sequences. *Bioinformatics* **18** 769-770.

[27] Muralidhar K, Chadha N & Kohli R 1988 Purification and characterization of prolactin from sheep and buffalo pituitaries. *Journal of Biosciences* **13** 201-214.

[28] Niemisto A, Dunmire V, Yli-Harja O, Zhang W & Shmulevich I 2005 Robust quantification of in vitro angiogenesis through image analysis. *Ieee Transactions on Medical Imaging* **24** 549-553.

[29] Panchal M & Muralidhar K 2008 Purification of monomeric prolactin charge isoform from buffalo pituitaries. *Preparative Biochemistry and Biotechnology* **38** 99-109.

[30] Panchal M. & Muralidhar K. 2010 Purification and biological characterization of bacterially expressed recombinant buffalo prolactin. *Prep. Biochem. Biotechnol*. **40** 276-285.

[31] Papkoff H, Gospodarowicz D, Candiotti A & Li CH 1965 Preparation of ovine interstitial cell-stimulating hormone in high yield. *Archives of Biochemistry and Biophysics* **111** 431-438.

[32] Schwede T, Kopp J, Guex N & Peitsc MC 2003 SWISS-MODEL: an automated protein homology-modeling server. *Nucleic Acids Research* **31** 3381-3385.

[33] Sinha YN 1995 Structure variants of prolactin: Occurrence and physiological significance. *Endocrinology Reviews* **16** 354-369.

[34] Staton CA, Stribbling SM, Tazzyman S, Hughes R, Brown NJ & Lewis CE 2004 Current methods for assaying angiogenesis *in vitro* and *in vivo*. *International Journal of Experimental Pathology* **85** 233-248.

[35] Struman I, Bentzien F, Lee H, Mainfroid V, D'Angelo G, Goffin V, Weiner RI & Martial JA 1999 Opposing actions of intact and N-terminal fragments of the human prolactin/growth hormone family members on angiogenesis: novel mechanism for the regulation of angiogenesis. *Proceeding of the National Academy of Sciences* **96** 1246-1251.

[36] Teilum K, Hoch JC, Goffin V, Kinet S, Martial JA & Kragelund BB 2005 Solution structure of human prolactin. *Journal of Molecular Biology* **351** 810-823.

[37] Towbin H, Staehelin T & Gordon J 1979 Electrophoretic transfer of proteins from polyacrylamide gels to nitrocellulode sheets: procedure and some applications. *Proceeding of the National Academy of Sciences* **76** 4350-4354.

[38] Wang YF & Walker AM 1993 Dephosphorylation of standard prolactin produces a more biologically active molecule: evidence for antagonism between nonphosphorylated and phosphorylated prolactin in the stimulation of Nb2 cell proliferation. *Endocrinology* **133** 2156-2160.

FIGURE LEGENDS

Figure 1. SDS-PAGE and immunoblot analysis of APP-I. A, Each protein was separated by 15 % gel under reducing condition. **B**, Immnuoblot of A. **C**, Calibration curve of APP-I, semi pure buPRL. Black arrow denotes buPRL monomer band (23.4 kDa), and grey arrows point to the band which shows approximately 18.4 kDa and 14.5 kDa on the calibration curve. **SDS-PAGE and immunoblot analysis. Each lane was loaded with 10 ug. D**, L1, APP-I; L2, buPRL monomer fraction from re-chromatography of APP-I; L3, APP-I 70; L4, APP-I 90-70. **E**, Immunoreactivity; L1', APP-I; L4', APP-I 90-70; M, Protein marker. **F**, Densitometry of M, L3 and L4 of D. Black arrow points monomer band. Grey arrows represent higher sized forms and light grey ones represent lower sized forms. Red arrow denotes the cleaved form.

Figure 2. Modified Papkoff's and Ellis'-Wilhelmi's protocols.

Figure 3. Antiangiogenic activity by *ex vivo* and *in vitro* assays. A, Results of CAM assay. Eggs at 6th day of incubation were

used for the assay. B, Analysis of the results of A. C, Results of endothelial cell migration assay. Values are means ± SEM. P < 0.05 vs control. **Significantly different from control cells (P < 0.001).

Figure 4. Immunoreactive assay of buPRL monomer and (AP)P-I 90-70 with buPRL antiserum.

Figure 5. ***In silico*** **analysis of buPRL monomer by ExPASy proteomics tools. A**, Predicted of Tyr-*O*-sulfate sites in buPRL monomer by Sulfinator. **B**, Predicted phosphorylation site in buPRL monomer by Netphos.

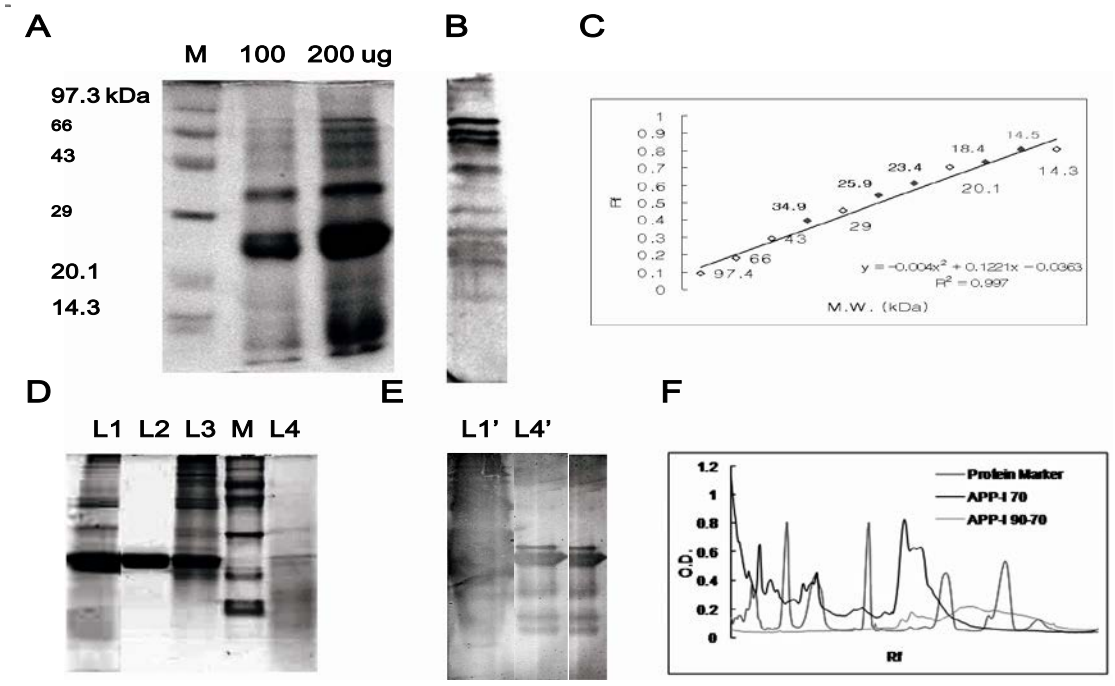

Figure 1

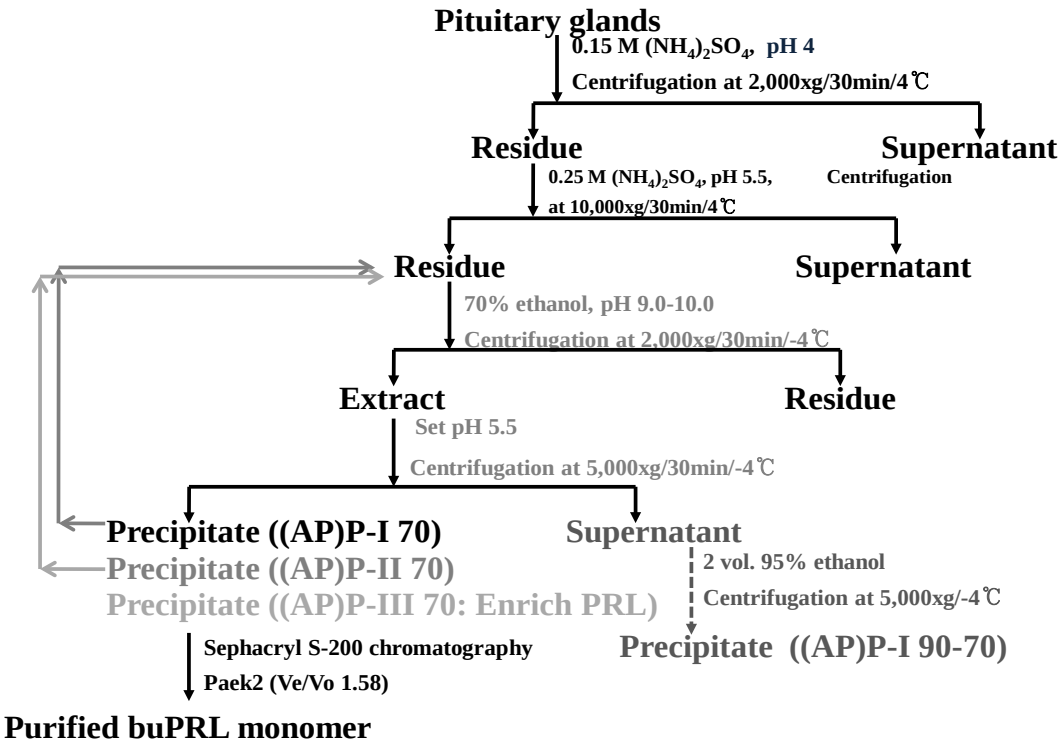

Figure 2

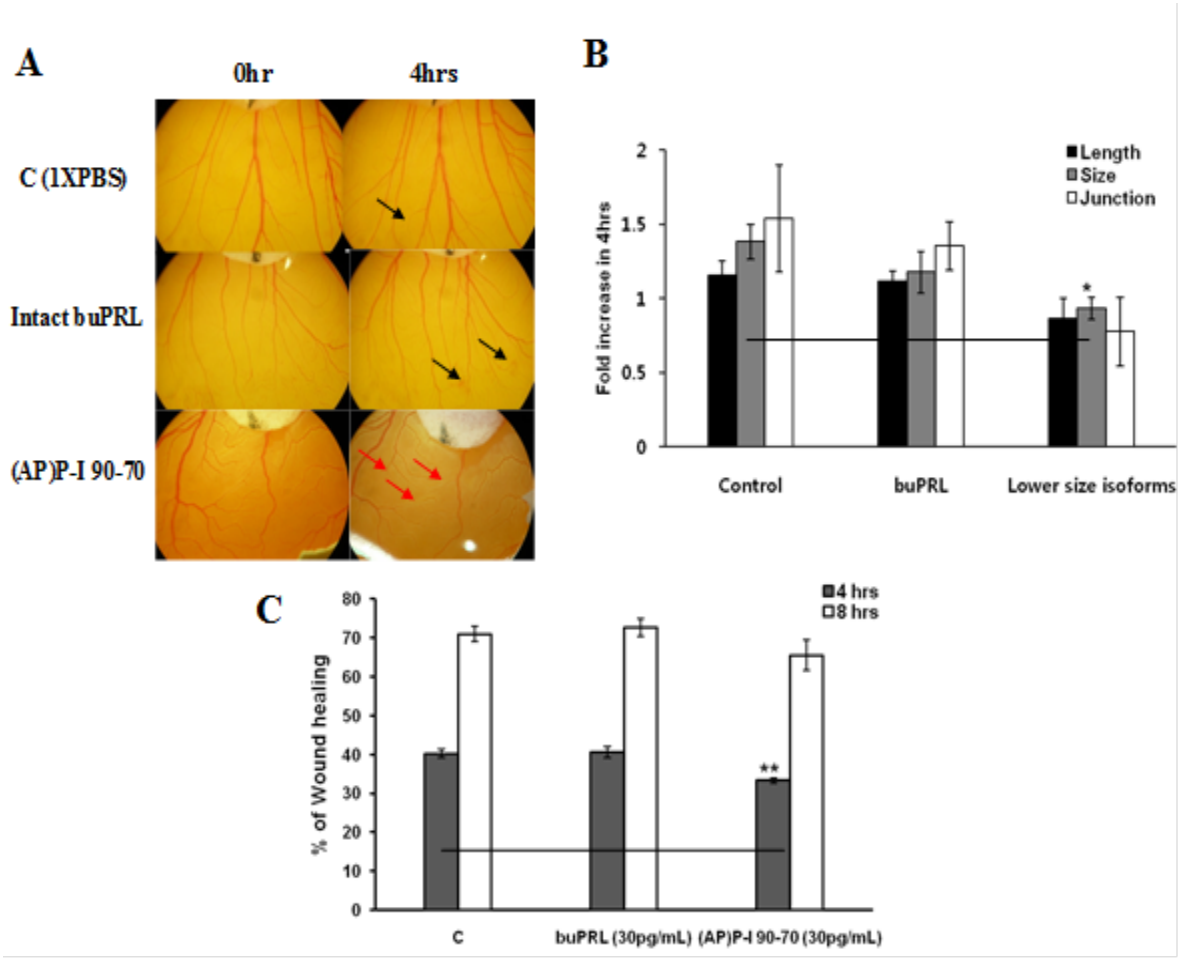

Figure 3

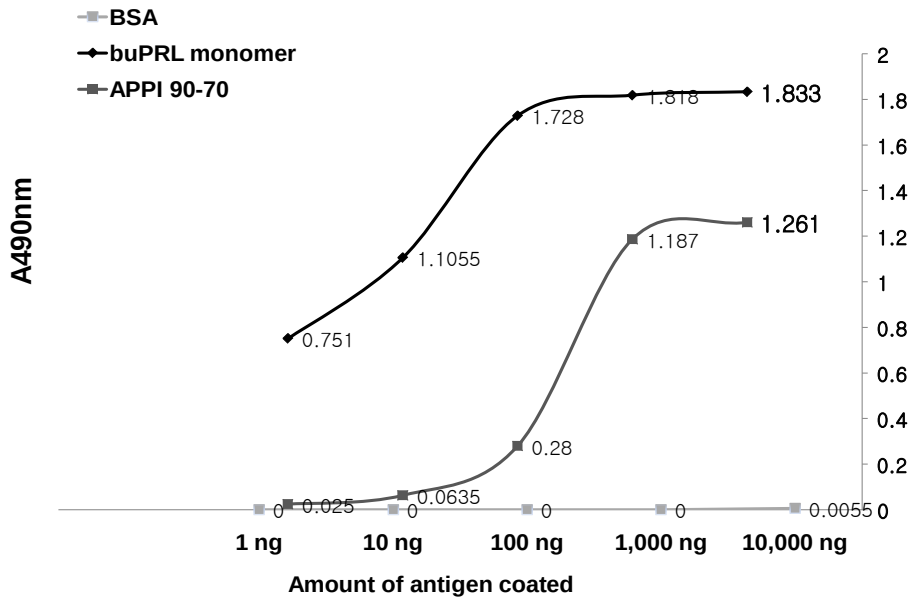

Figure 4

Table 2: Immunoreactive Assay Result of buPRL Monomer and (AP)P-I 90-70 with buPRL Antiserum

	Value	
Parameter	**buPRL monomer**	**(AP)P-I 90-70**
ED50	**4 ng**	**140 ng**
Vmax (Absorbance at 10,000 ng)	**1.833**	**1.261**

ED, effect dose.

A

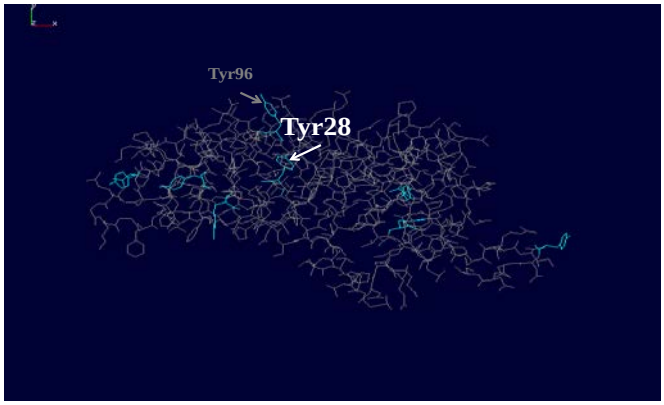

B

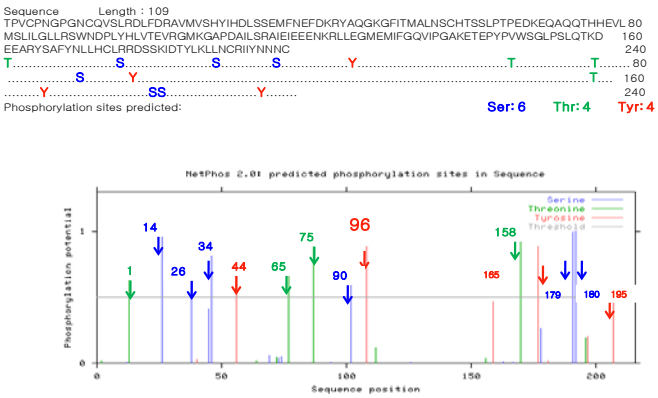

Figure 5